

## Effects of the Tibetan Plateau on the onset of the summer monsoon in South Asia: The role of the air-sea interaction

Manabu Abe,<sup>1,5</sup> Masatake Hori,<sup>2</sup> Tetsuzo Yasunari,<sup>3</sup> and Akio Kitoh<sup>4</sup>

Received 28 May 2012; revised 18 January 2013; accepted 18 January 2013; published 18 January 2013.

[1] Using both a coupled atmosphere-ocean general circulation model (GCM) and an atmospheric GCM, we investigate the effects of the Tibetan Plateau (TP) on the onset of the South Asian summer monsoon by conducting simulations with and without the TP. In the coupled GCM, the presence of the TP causes the monsoon onset to occur approximately 15 days later in the Arabian Sea (AS) and India (ID) and approximately 10 days earlier in the Bay of Bengal (BB). These changes are attributed to different atmospheric circulation patterns and different conditions within the adjacent oceans, such as the AS and the BB. When the TP is included, lower sea surface temperatures (SSTs) in the AS contribute to a stable lower atmosphere, which suppresses convection over the AS and ID in May. In contrast, low pressure over South Asia, caused by the TP, induces a southwesterly toward the BB that transports a substantial amount of water vapor to the BB. This flow results in an earlier monsoon in the BB. Without the TP, higher SSTs that are formed in the AS in May destabilize the lower atmosphere and create a depression, resulting in an earlier onset of the monsoon over the AS and ID. Consequently, the cyclonic circulation spreads abruptly to the BB, and precipitation begins to increase over the BB. Therefore, the air-sea interaction in the adjacent ocean under the influence of the TP strongly modulates the onset of the South Asian summer monsoon. This modulation was verified by the atmospheric GCM experiments.

**Citation:** Abe, M., M. Hori, T. Yasunari, and A. Kitoh (2013), Effects of the Tibetan Plateau on the onset of the summer monsoon in South Asia: The role of the air-sea interaction, *J. Geophys. Res. Atmos.*, 118, 1760–1776, doi:10.1002/jgrd.50210.

### 1. Introduction

[2] The South Asian summer monsoon is characterized by heavy precipitation, a southwesterly flow in the lower troposphere, and anticyclonic circulation in the upper troposphere. The circulation of the Asian monsoon is regulated by the Tibetan Plateau (TP). The TP works as an obstacle directing zonal circulation in the lower troposphere. Westerly winds from west of the TP are diverted and become northwesterly winds in South Asia. In addition, orographically enhanced rainfall occurs on the windward side of the TP, with rainshadow drying on its lee side. Furthermore, because the surface of the TP is located in the middle troposphere, the TP heats the middle troposphere directly. This heating reverses the meridional temperature gradient of the middle-

upper troposphere over South Asia during the spring and summer. This reversal intensifies the Asian summer monsoon circulation. The heating effect is also significantly associated with the timing of the Asian summer monsoon [e.g., *Li and Yanai*, 1996; *Ueda and Yasunari*, 1998]. *Minoura et al.* [2003] reported that an increase in the surface temperature and dry intrusion in the 600–850 hPa layer over the Arabian Sea (AS), the Bay of Bengal (BB), and the Indian subcontinent (ID) can play a crucial role in enhancing convective instability prior to the onset of the Indian summer monsoon.

[3] Summer monsoon precipitation tends to begin at different times on the Indochina Peninsula, the South China Sea, the BB, the ID, the AS, and the western Pacific; this asynchronicity reflects the developmental processes of the Asian summer monsoon [e.g., *Wu and Zhang*, 1998; *Wang and LinHo*, 2002]. Generally, in South Asia, the monsoon rainy season in the BB and the AS begins in early and late May, respectively. The monsoon rains then advance to the ID. The monsoon rainy season in Southeast Asia begins in the middle of May and gradually migrates north to East Asia in late May and June. The monsoon rainy season generally begins over the tropical western Pacific in June. The summer monsoon rains spread progressively and systematically once the onset phases have occurred.

[4] Previous studies have investigated the effects of the TP on the climate of the Asian summer monsoon by using atmospheric or coupled general circulation models (AGCM or CGCM) [e.g., *Hahn and Manabe*, 1975; *Kutzbach et al.*,

<sup>1</sup>Graduate School of Environmental Studies, Nagoya University, Nagoya, Japan.

<sup>2</sup>Research Institute for Global Change, Japan Agency of Marine-Earth Science and Technology, Yokosuka, Japan.

<sup>3</sup>Hydrospheric and Atmospheric Research Center, Nagoya University, Nagoya, Japan.

<sup>4</sup>Meteorological Research Institute, Tsukuba, Japan.

<sup>5</sup>Now at Arctic Environment Research Center, National Institute of Polar Research, Tachikawa, Tokyo, Japan.

Corresponding author: M. Abe, Arctic Environment Research Center, National Institute of Polar Research, 10-3, Midori-machi, Tachikawa, Tokyo, 190-8518, Japan. (abe.manabu@nipr.ac.jp)

©2013. American Geophysical Union. All Rights Reserved.  
2169-897X/13/10.1002/jgrd.50210

1989, 1993; *Abe et al.*, 2003, 2004; *Kitoh*, 2004]. Many studies have investigated the effect of large-scale orography on the Asian monsoon over a mean seasonal time scale, and others have investigated the effect of the TP on the onset of the summer monsoon in Asian regions. *Hahn and Manabe* [1975] investigated the effect of mountains on the South Asian monsoon with the AGCM, revealing that, in a model that included mountains, a humid southwesterly flow near the surface extended abruptly from the equatorial latitudes to the South Asian low pressure belt centered at 30°N. However, in a model without mountains, this flow did not extend as far northward as northern and central India. *Chakravorty et al.* [2006] investigated the impact of orography in different regions of the Earth on the onset of the Indian summer monsoon (ISM) using an AGCM and reported that an early onset of the ISM occurred in response to the removal of the African orography. *Kitoh* [2004], using the same CGCM as the present study, reported that the Baiu rainband appeared only when the mountain elevation was greater than 60% of the current elevation and that the northward propagation of this rainband was simulated in cases with mountains higher than 60% of the current elevation. Because an experiment with CGCM allows the ocean state to change via the removal of the orography [*Kitoh*, 1997; *Abe et al.*, 2003, 2004; *Okajima and Xie*, 2007], the air-sea interaction that is associated with an evolution of the South Asia monsoon without the TP in the CGCM must be different from that in the AGCM, resulting in a different timing of the onset of the South Asian summer monsoon than that in the presence of the TP. However, no previous study has investigated the effect of the TP on the onset of the South Asian summer monsoon using the CGCM, although this effect was investigated with the AGCM by *Hahn and Manabe* [1975] and *Chakravorty et al.* [2006]. Therefore, in the present study, we investigate differences in the onset of the South Asian summer monsoon between cases with and without the TP using the CGCM. We discuss the effect of the air-sea interaction that is associated with the presence of the TP on the geographical features of the onset date of the South Asian summer monsoon as well as the mechanism that triggers the onset of the monsoon, by comparing the CGCM and AGCM runs.

**2. Model and Experimental Design**

[5] We used a coupled atmosphere-ocean general circulation model (MRI GCM2.3.2b) [*Yukimoto et al.*, 2001]. The AGCM was developed based on a version of the operational weather forecasting model that was developed by the Japan Meteorological Agency (JMA). The details of the AGCM are described in *Shibata et al.* [1999]. The horizontal resolution of the AGCM is T42 in wave truncation (approximately 2.8° × 2.8° in longitude and latitude), and the vertical configuration consists of a 30-layer sigma-pressure hybrid coordinate with a maximum of 0.4 hPa. The parameterization of the deep, moist convection follows the Arakawa-Schubert scheme with prognostic closure. The oceanic GCM (OGCM) is a Bryan-Cox type GCM with a horizontal resolution of 2.5° longitude and 2.0° latitude. The meridional resolution between 4°S and 4°N is finer to more accurately resolve the equatorial oceanic waves. The OGCM has 23 vertical levels, with the deepest at 5000 m. *Yukimoto et al.* [2001] described the model climate when a flux adjustment was applied, and

*Rajendran et al.* [2004] investigated the Asian summer monsoon and its variability. *Kitoh* [2004, 2007] also investigated the sensitivity of the Asian summer monsoon and the El Niño–Southern Oscillation (ENSO) to mountain uplift with the same model.

[6] We conducted two runs with the CGCM: TP100 and TP00. TP100 was integrated over 50 years with a realistic land-sea distribution and orography. In TP00, the orography greater than 200 m within the Asian region was removed so that the altitude of the land surface was 200 m. Figure 1 displays the topographic maps of TP100 and TP00. This design is different from that used by *Kitoh* [2004, 2007], in which global orography was removed in the no-mountain case. TP00 was also integrated over 50 years with the same initial condition as TP100. In addition, to validate the effect of the ocean change resulting from the removal of the TP, we conducted three AGCM runs, labeled AT00, AT100, and AT100+O00. AT00 and AT100 included the same orographic conditions as TP00 and TP100, respectively. In both of the AGCM runs, sea surface temperatures (SSTs) averaged over the last 20 years within TP100 were prescribed as the climatological SSTs for all of the model years. The AT100+O00 run also included the TP. However, in the AT100+O00 run, the SSTs averaged over the last 20 years within TP00 were prescribed. All of the AGCM runs were integrated over 30 years. In this analysis, we used climatological

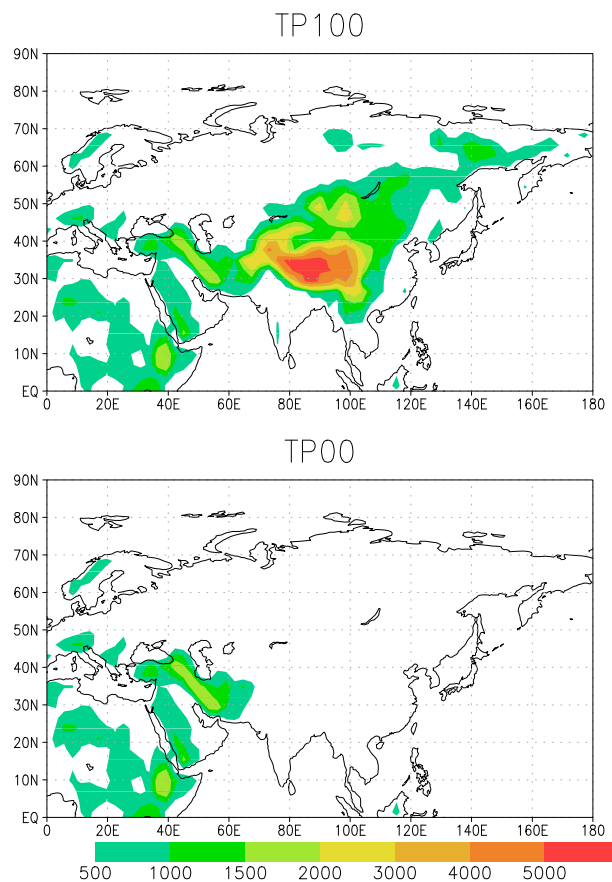


**Figure 1.** The orographies prescribed in TP100 and TP00. The same orographies were also prescribed in AT100 and AT00, respectively. Data are shown in meters.

5-day mean data that were averaged over the last 20 model years (31–50) within the CGCM runs and over the last 10 model years (21–30) within the AGCM runs.

### 3. Model Performance

[7] Figure 2 illustrates the biases in mean precipitation, wind at 850 hPa, and SST for the GCM during the boreal spring (March–April–May) and summer (June–July–August). In this bias analysis, we used data from the Climate Prediction Center (CPC) merged Analysis of Precipitation (CMAP) [Xie and Arkin, 1997] for precipitation, reanalysis data from the European Centre for Medium-Range Weather Forecasts (ECMWF) [Uppala et al., 2005] for wind at 850 hPa, and the National Oceanic and Atmospheric Administration's (NOAA) optimum interpolated SST (OISST) V2 data provided by NOAA/OAR/ESRL PSD (Boulder, Colorado, USA (<http://www.esrl.noaa.gov/psd/>)) [Reynolds et al., 2002]], for SST. In addition, the CMAP data, the ERA40 data, and

the OISST data were averaged arbitrarily for 1981–2005, 1971–2000, and 1993–2005, respectively. The GCM simulates the mean spring precipitation and wind at 850 hPa reasonably well, although small biases for precipitation and wind at 850 hPa are present. The simulated spring mean precipitation is slightly overestimated for the BB and Southeast Asia. In addition, the simulated westerly winds at 850 hPa over the southern BB are stronger than those in ERA40. Compared with these biases over Southeast Asia, the precipitation and wind data at 850 hPa over South Asia are well simulated. However, the biases in the mean summer precipitation and wind at 850 hPa are larger than those for the spring mean. The mean summer precipitation over the western region of the BB is overestimated, whereas that over the northern region of the BB is underestimated. The westerly winds from the AS to Southeast Asia and the ID are weaker than those in ERA40. In contrast, the westerly winds over the southern BB are stronger. These biases indicate that the summer monsoon westerly winds in the low troposphere are less realistic.

[8] Comparing the observations of the seasonal progression of precipitation and wind at 850 hPa to the CGCM data, Figure 3 illustrates a longitude-time cross section, for the mean pentad precipitation and wind at 850 hPa, averaged for 10°N–20°N. From November to February, weak easterly winds blow over South and Southeast Asia. During March, the systematic wind disappears. This seasonal change in the simulated low tropospheric wind over South Asia corresponds to that in ERA40. The simulated monsoon's southwesterly flow in the BB begins in early May, which corresponds closely with ERA40. The simulated northwesterly flows during May in the AS and ID are also similar to those in ERA40. The increased precipitation above 4 mm d<sup>-1</sup> in the BB in the CGCM begins in mid-April, which is quite close to the date in the CMAP, although the increased precipitation in the AS and the ID occurs approximately 10 days later in the CGCM. However, greater precipitation in early June over the AS does not occur in the CGCM. In May, the northwesterly flows over the AS and ID are stronger than those in ERA40. This stronger northwesterly wind is related to the later onset of the monsoon in the ID and reduced precipitation in early June over the AS in addition to the cold biases in SSTs. Furthermore, the CGCM was not able to realistically simulate the climatological intraseasonal variations, such as the breaks in the monsoonal precipitation and the low-level wind in South Asia [e.g., Takahashi and Yasunari, 2006]. These discrepancies in climatological intraseasonal variation in the CGCM are beyond the scope of the present study, which is the onset of the South Asian monsoon.

[9] The CGCM realistically simulated ocean surface currents and SSTs; Figure 4 illustrates the monthly mean ocean surface currents and SSTs from March to June for the observed data and for the CGCM. We used near-real-time data for ocean surface currents that were derived from satellite altimeter and scatterometer data [Bonjean and Lagerloef, 2002] and the National Oceanic and Atmospheric Administration's (NOAA) optimum interpolated SST (OISST) V2 data that were provided by NOAA/OAR/ESRL PSD, Boulder, Colorado, USA (<http://www.esrl.noaa.gov/psd/>) [Reynolds et al., 2002]. These observations were averaged from 1993 to 2005.

[10] The CGCM simulated westward and eastward ocean surface currents north and south of the Equator during March and April, respectively. A systematic current over

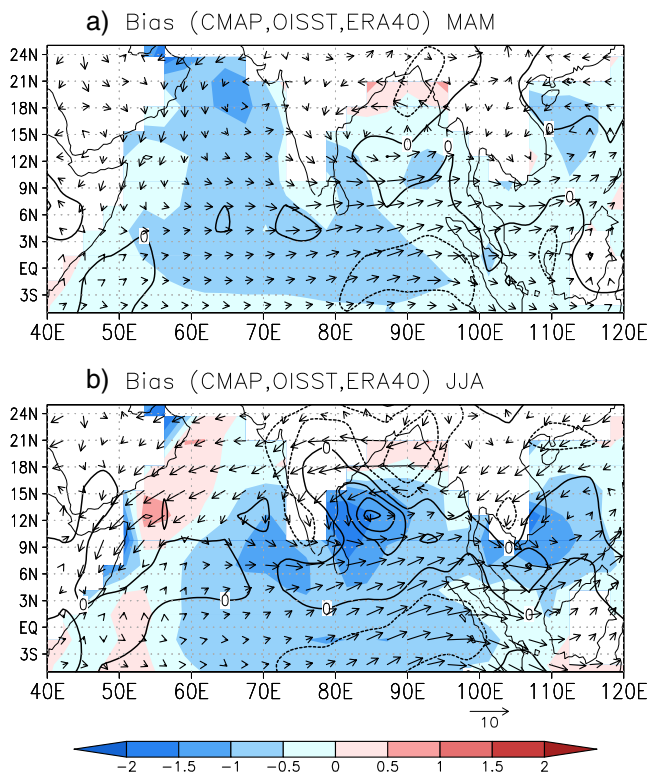


**Figure 2.** Biases for precipitation, wind at 850 hPa, and sea surface temperature (SST), indicating the March–April–May and June–July–August means. Data from the Climate Prediction Center (CPC) merged Analysis of Precipitation (CMAP) [Xie and Arkin, 1997] for precipitation, reanalysis data from the European Centre for Medium-Range Weather Forecasts (ECMWF) [Uppala et al., 2005] for wind at 850 hPa, and the National Oceanic and Atmospheric Administration's (NOAA) optimum interpolated SST (OISST) V2 data [Reynolds et al., 2002] for SST were used as the realistic data. The CMAP data, the ERA40 data, and the OISST data were averaged arbitrarily for 1981–2005, 1971–2000, and 1993–2005, respectively. The units for precipitation, wind, and SST are mm d<sup>-1</sup>, m s<sup>-1</sup>, and K, respectively.

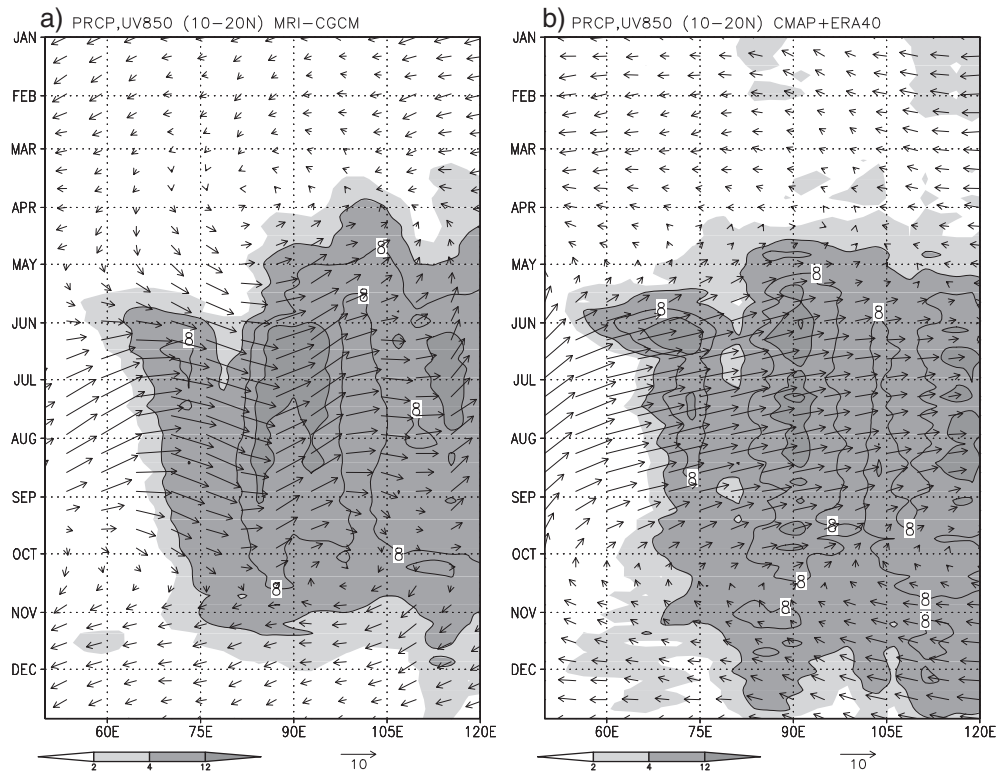


**Figure 3.** A longitude-time cross-section of precipitation and wind at 850 hPa in TP100 and the observed data. For the observations, precipitation and wind are from CMAP and ERA40, respectively. The units of precipitation and wind are  $\text{mm d}^{-1}$  and  $\text{m s}^{-1}$ , respectively. The CMAP and ERA40 were averaged for 1981–2005 and 1971–200, respectively.

the AS and the BB during these months did not occur in either the CGCM or the observations. In addition, during these months, the simulated SST distribution in the Indian Ocean, AS, and BB is similar to the observed SSTs, although the simulated SSTs were lower (Figure 2). In May and June, the simulated clockwise ocean surface currents in the western equatorial Indian Ocean are consistent with the observed currents. The eastward current along the Equator that is simulated in the CGCM also matches the observed data. Furthermore, the CGCM simulates eastward currents in the AS and BB, which are similar to the observed currents. The simulated SST distribution is similar to the observed distribution during these months, although the SSTs are lower in TP100 than the observed SSTs (Figure 2). Furthermore, because the precipitation biases in the spring means are not extreme, the lower SSTs are unlikely to strongly affect spring precipitation. However, because precipitation over the southern part of the BB and the South China Sea is overestimated during summer, the outstanding negative biases in SSTs may be attributed to less incoming shortwave radiation to the surface due to increased cloud cover (Figure 2).

## 4. Results

### 4.1. The Onset Date of the Summer Monsoon Precipitation

[11] To objectively determine the onset date of the South Asian summer monsoon precipitation in the

GCM runs, we employed a definition used by *Wang and LinHo* [2002] (hereafter WL02), in which the onset date was defined as the date when the difference in the monthly mean precipitation in January (hereafter  $\Delta P$ ) is greater than  $4 \text{ mm d}^{-1}$ .

[12] Figure 5 displays the geographical distribution of the onset date in the TP100 and TP00 runs. The distribution of the onset date for TP100 is close to the observed onset date that is displayed in Figure 6 of WL02 (Figure 5a). The simulated monsoon rainy season advances from the BB, to the northern part of the ID, through the southern part of the ID. The onset dates in the AS and the ID for TP100 are late May to early June (Pentad number (P) 26–29) and middle to late June (P32–36), respectively. However, the onset in the Indochina Peninsula occurs first in late April (P16–18) in TP100, approximately 1 month earlier than in the observations. The onset in the BB also occurs approximately 10 days earlier than the observed date. In addition, the onset in ID is delayed by approximately 10 days compared to the observations. Although these discrepancies in the onset timing over the BB, Southeast Asia, and ID were found, the CGCM can simulate realistic advances of the South Asian summer monsoon rainband.

[13] As shown in Figure 5b, the onset dates for the various geographic regions in TP00 differ from those in TP100. The onset in the AS and the BB in TP00 occur in late April to mid-May (P24–28) and late May to early June (P28–30), respectively; the onset date in the AS is earlier than that in the BB in TP00, whereas this pattern is reversed in TP100.

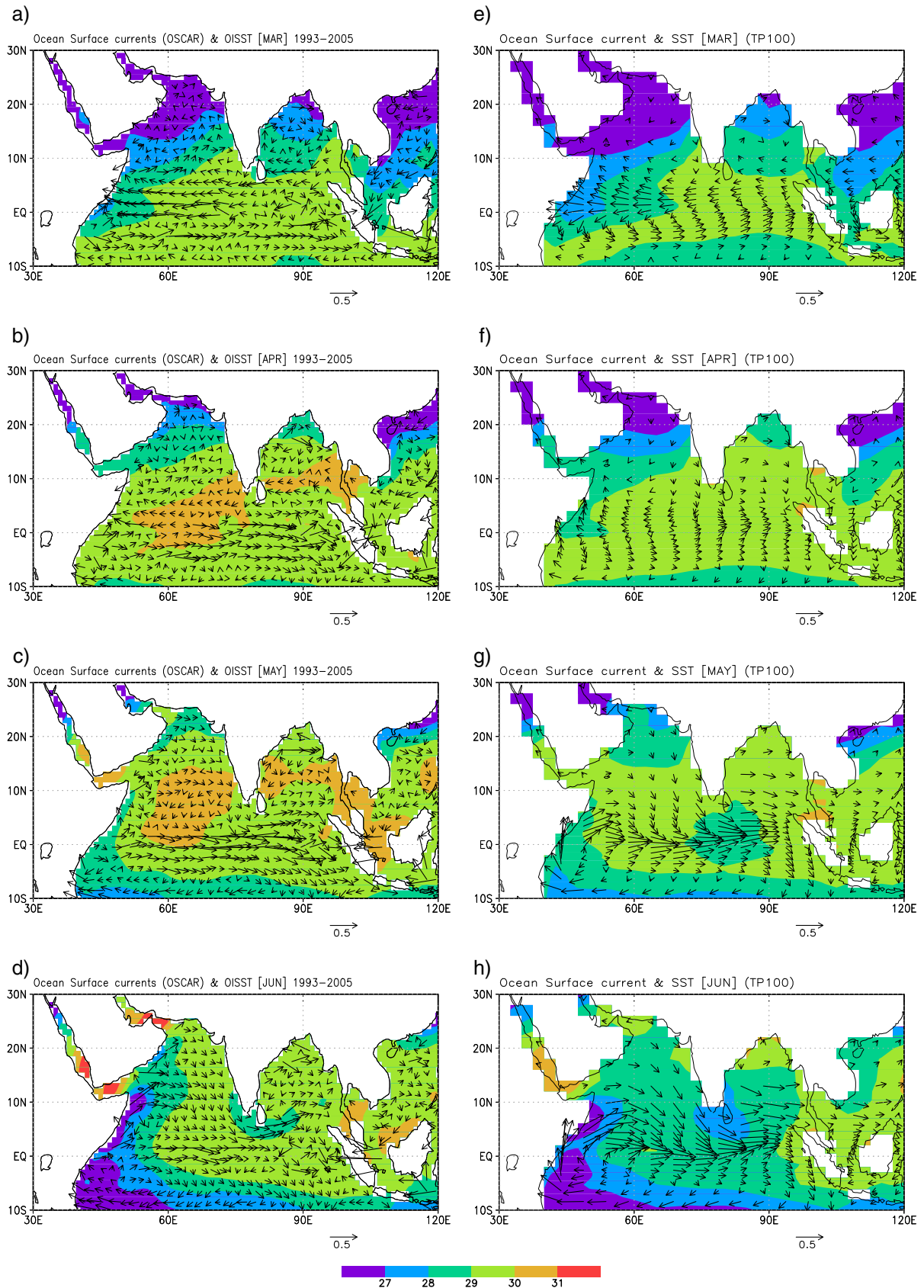


**Figure 4.** (a–d) The monthly mean ocean surface current, derived from the satellite and sea surface temperature (SST), during March to May. (e–h) The monthly mean ocean surface current and SST in TP100 during March to May. The units of ocean current and SST are  $\text{m s}^{-1}$  and  $^{\circ}\text{C}$ , respectively.

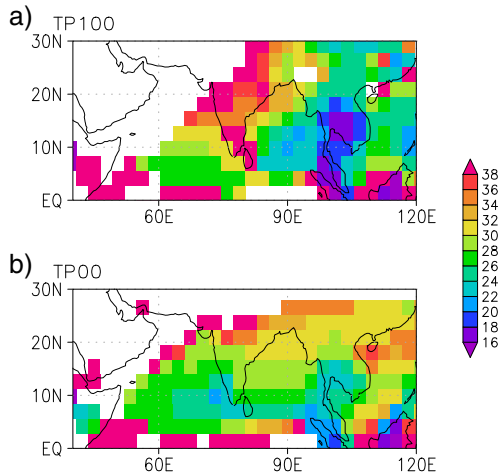


**Figure 5.** A geographical map of the onset date for summer precipitation in TP100 (a) and TP00 (b). The values represent pentad numbers for the onset date.

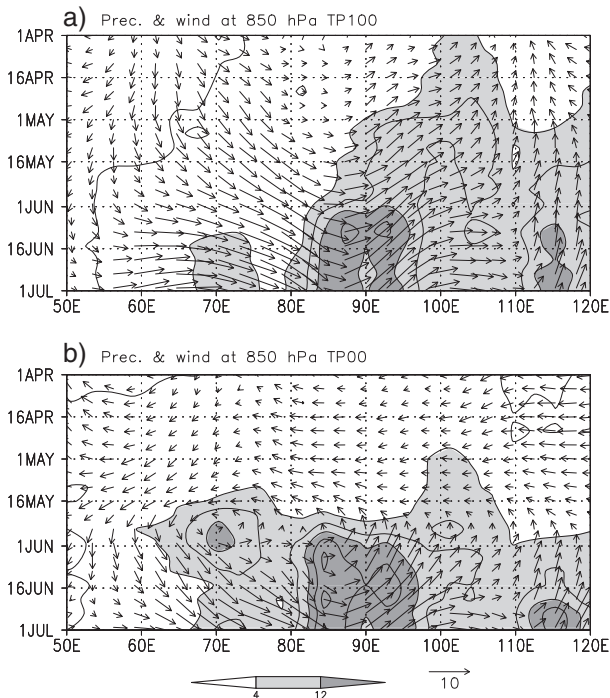


**Figure 6.** Longitude-time cross sections of the precipitation differences from the January mean precipitation for TP100 ( $\Delta P$ ) and the wind at 850 hPa, averaged over the region  $10^{\circ}\text{N}$ – $20^{\circ}\text{N}$ . The top represents TP100, and the bottom represents TP00. The  $\Delta P$  greater than  $4 \text{ mm d}^{-1}$  is shaded. The vectors indicate the wind. The units of the  $\Delta P$  and wind are  $\text{mm d}^{-1}$  and  $\text{m s}^{-1}$ , respectively.

Furthermore, the monsoon area over the AS is larger in TP00 than in TP100.

#### 4.2. The Difference in the Evolution of the South Asian Summer Monsoon

[14] To clearly describe the difference between the onset of the South Asian monsoon in TP100 and TP00, Figure 6

illustrates the longitude-time cross sections of the  $\Delta P$  and wind at 850 hPa for TP100, averaged for  $10^{\circ}\text{N}$ – $20^{\circ}\text{N}$ , in South Asia from April to August.

[15] The seasonal change in precipitation in South Asia in TP100 is quite different from that in TP00. In TP100, the  $\Delta P$  greater  $4 \text{ mm d}^{-1}$  in the Indochina Peninsula (approximately  $100^{\circ}\text{E}$ ) first appears in early April, whereas in the BB (approximately  $85^{\circ}\text{E}$ ), it first appears in mid-May. The southwesterly flow at 850 hPa appears in Southeast Asia at the same time as the start of the  $\Delta P$  above  $4 \text{ mm d}^{-1}$ . However, the  $\Delta P$  above  $4 \text{ mm d}^{-1}$  in the BB and the Indochina Peninsula appears later in TP00; the onset in the Indochina Peninsula and the BB occur earlier in TP100 than in TP00 due to the presence of the TP. In contrast, before early June, there is no  $\Delta P$  above  $4 \text{ mm d}^{-1}$  in ID (approximately  $75^{\circ}\text{E}$ ) or the AS (approximately  $65^{\circ}\text{E}$ ) in TP100, whereas the northwesterly flow appears in late April and gradually grows stronger until reaching the BB. Beginning in late June in TP100, the southwesterly flow begins to appear in the AS at the same time as the onset of precipitation above  $4 \text{ mm d}^{-1}$ . This result suggests that the TP delays the onset of the monsoon precipitation in the AS and ID, whereas in TP00, without the presence of the TP, precipitation in the AS and ID increases beginning in late May (about P26).

[16] TP100 and TP00 exhibit different wind patterns at 850 hPa in early April to May, before the onset of the monsoon in South Asia (Figure 6). To compare the spatial features of the evolution in the lower-level circulation of the Asian summer monsoon during April to May, Figure 7 illustrates the seasonal changes in the climatological geopotential height and moisture transportation at 850 hPa and evaporation minus precipitation ( $E - P$ ) in TP100 and TP00. During April to May in TP00, subtropical anticyclonic circulation appears in South Asia, seeming to extend from the Pacific through the ID to the AS (Figure 7). Because solar irradiance in the tropical-subtropical region of the Northern Hemisphere is greater in the early spring, the thermal contrast between the surface temperatures of the land and sea in South Asia becomes stronger. Therefore, a higher pressure field only at the lower troposphere appears over the oceans of the AS and the BB (Figure 7). After that time, in mid-May, the cyclonic circulation evolves rapidly to initiate monsoon precipitation in the AS and ID. This abrupt onset accompanies an increase in precipitation over all of South Asia for a short time, after which the monsoon begins in the BB. Furthermore, the pressure reduction over the AS induces the Somali Jet (a southerly flow along the East African coast over the equatorial western Indian Ocean) to transport a substantial amount of water vapor into the AS and the southern region of the ID (Figures 7i and 7j). The transported water vapor strongly contributes to the early onset of precipitation in the AS and the ID. In contrast, during April to May in TP100, lower pressure fields to the south of the TP are formed under the influence of the TP [Hahn and Manabe, 1975]. In this scenario, a drier northwesterly flow through the AS into the ID suppresses the convective activity over the AS and ID, delaying the onset of the monsoon precipitation over the AS and ID. In contrast, a moist southwesterly flow begins to induce greater precipitation in Southeast and East Asia. Therefore, the results indicate that the presence of the TP creates an east-west contrast, with a later onset of the monsoon

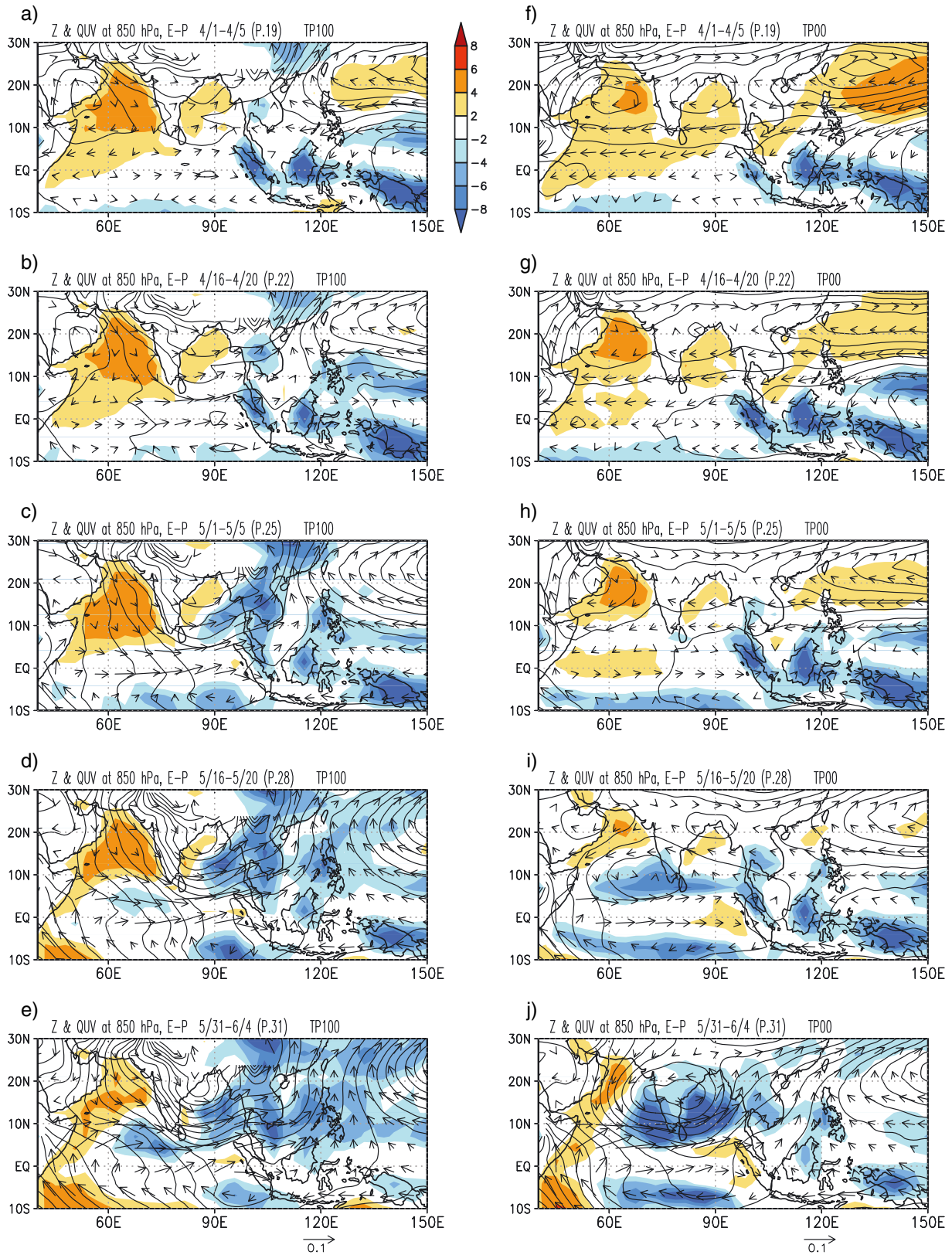


**Figure 7.** Seasonal changes in the spatial distribution of the geopotential height (contours), moisture transportation at 850 hPa (vector), and evaporation minus precipitation ( $E - P$ ) (shade) for TP100 and TP00. The left and right columns are for TP100 and TP00, respectively. Figures from top to bottom in both columns list data for 1–5 April, 16–20 April, 1–5 May, 16–20 May, and 31 May to 4 June. The units of geopotential height, wind, and  $E - P$  are m,  $\text{kg m kg}^{-1} \text{s}^{-1}$ , and  $\text{mm d}^{-1}$ , respectively. For geopotential height, the data were spatially smoothed to facilitate an understanding of the features of the geopotential heights around the Tibetan Plateau.

in South Asia and an earlier onset in Southeast Asia, even at the same latitude.

[17] Previous studies have reported that a weakening or a reversal of the meridional temperature gradient in the upper troposphere plays a substantial role in the onset of the Asian summer monsoon [e.g., *Li and Yanai, 1996; Ueda and Yasunari, 1998; Inoue and Ueda, 2011*]. In the present study, we analyzed the meridional temperature gradient (MTG) at 300 hPa, similar to *Inoue and Ueda [2011]*. Figures 8a and 8b depict the changes in the temperature at 300 hPa over Asia from the premonsoon season to the monsoon season in TP100 and TP00, respectively. Both of these figures display an increase in temperature over the continent. In TP100, remarkable increases of greater than 4°C occur over the TP, weakening the MTG over South Asia. In addition, remarkable temperature increases in TP00 are located slightly farther south than in TP100. Although the increase in TP00 is weaker than in TP100, the MTG in TP00 is weakened over South Asia. Figure 8c compares the seasonal evolutions of the upper tropospheric MTG in TP100 and TP00. Here MTG is defined as the area-averaged 300-hPa temperature differences over the continent (TP100: 20°N–40°N, 50°E–100°E; TP00: 15°N–35°N, 50°E–100°E) and over the northern Indian Ocean (TP100: 0°N–20°N, 50°E–100°E; TP00: 5°S–15°N, 50°E–100°E). The differences in the area between TP100 and TP00 are due to the remarkable MTG increase in TP00, which is found slightly farther to the south than in TP100. In TP100, the negative MTG increases gradually as the season advances from boreal spring to summer. In contrast, the MTG in TP00 is slightly lower than in TP100 during April to early May and

then begins to increase in mid-May, when the monsoon precipitation over South Asia occurs in TP00. This result indicates that the upper troposphere was heated by the latent heat release of the convective activity, even in the case without the direct heating caused by the TP. Because the MTG in TP00 closely resembles that in TP100, the impact of the presence of the TP on the seasonal evolution of the MTG is unclear.

[18] To examine the relationship between the evolution of the geopotential height at 850 hPa, water vapor flow, SSTs, and precipitation, Figure 9 displays the time-latitude cross sections for these parameters in both the AS (65°E–75°E) and BB (85°E–95°E) for TP100 and TP00. In TP00, the geopotential height at 850 hPa over the AS is sharply reduced from early May to early June, with accompanying SSTs above 29°C in the AS. An increase in precipitation also begins in early May, with a larger increase occurring at approximately 9°N in late May. The precipitation is also consistent with the strength of the convergence of the water vapor flow. This enhancement of the increase in precipitation occurs at latitudes with the largest meridional gradient in SSTs. The large meridional gradient in SSTs causes the formation of the meridional gradient in the lower-tropospheric pressure field. This effect results in enhanced water vapor flow from the south and water vapor convergence, which causes the increase in precipitation. Therefore, both the higher SSTs and the corresponding large meridional gradient of SSTs over the southern part of the AS are principal factors causing the abrupt depression and convergence of water vapor over the AS in TP00. However, over the BB in TP00, the precipitation in the southern BB increases over higher SSTs in early May and then spreads northward, with higher SSTs during late

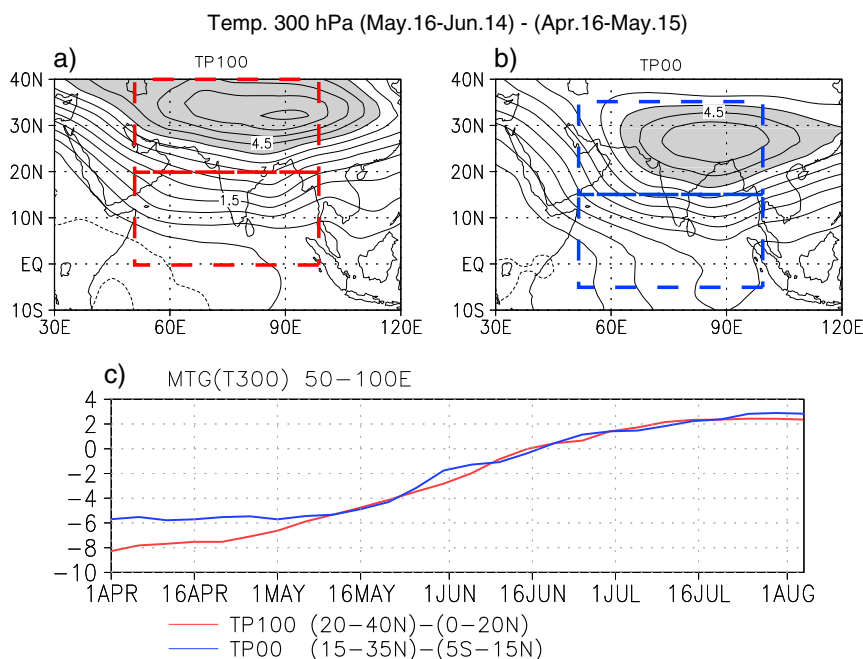


**Figure 8.** (a, b) Seasonal changes (16 May to 14 Jun minus 16 Apr to 15 May) in the 300 hPa temperatures in TP100 and TP00. Temperature increases of more than 4.0 K are shaded. (c) Seasonal evolutions in the meridional temperature differences at 300 hPa in TP100: [average of 20°N – 40°N, 50°E – 100°E] minus [average of 0°N – 20°N, 50°E – 100°E] and in TP00: [average of 15°N – 35°N, 50°E – 100°E] minus [average of 5°S – 15°N, 50°E – 100°E]). Temperatures at 300 hPa were averaged for each area, as indicated by the dashed line in Figures 8a and 8b.

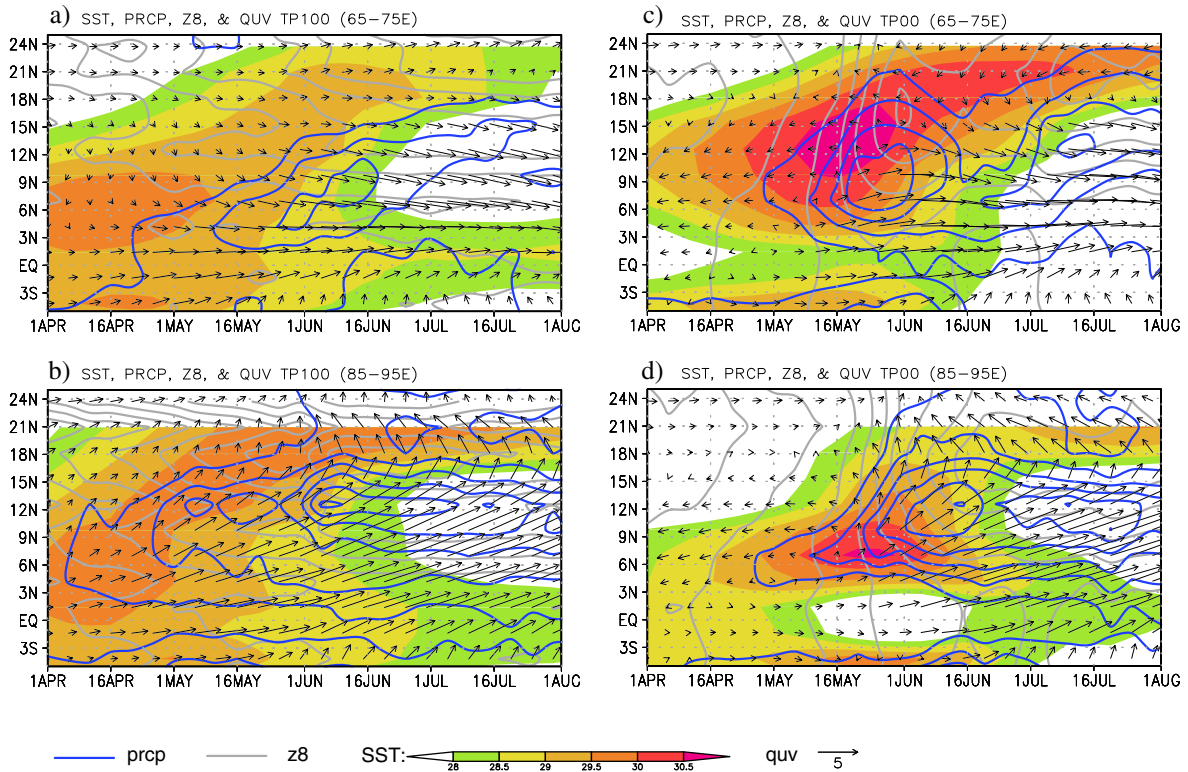


**Figure 9.** Time-latitude cross sections of the geopotential height at 850 hPa, column-integrated water vapor flow, precipitation, and sea surface temperature (SST) for the AS (65°E–75°E) and the BB (85°E–95°E) regions. Left: from TP100; bottom: from TP00. The shaded area indicates the sea surface temperature. Blue contours indicate the precipitation, with an interval of 4 mm d<sup>-1</sup>. Gray contours indicate the geopotential height at 850 hPa, with an interval of 100 m. Vectors indicate the column integrated water vapor flow. The units of geopotential height, water vapor flow, precipitation, and SST are m, m, kg m/kg s, mm d<sup>-1</sup>, and °C, respectively.

May to early June. Although the increase in precipitation during May is consistent with SSTs above 29°C, the precipitation over the BB in late May increases markedly due to the increase in the water vapor that is transported from the south. This increase indicates an enhancement of the precipitation increase over the BB, which is caused by the increase in water vapor transported from the south (Figures 6 and 9). Therefore, in TP00, because less water vapor is carried into the BB prior to late May, the onset of the monsoon precipitation over the BB is delayed. Consequently, in this GCM, incoming water vapor is a principal factor governing the onset of the monsoon precipitation in each region. In addition, the timing of the convergence of water vapor flow is related not only to higher SSTs but also to the spatial gradient of SSTs.

[19] In TP100, the geopotential height at 850 hPa in both the AS and BB decreases in April due to the presence of the TP. Subsequently, the geopotential height continues to decrease during May and June. This decrease is centered at the BB, where the SST is above 29°C during April and May and is higher than that in TP00. The increase in precipitation during April to May is also consistent with SSTs above 29°C. In addition, because of developing low-pressure fields over the BB due to presence of the TP, the southwesterly flow to the BB transports a significant amount of water vapor to the BB. This water vapor then converges

and increases the precipitation over the BB. In contrast, over the AS, although northward shifts in SSTs above 29°C are found during May to June, the SSTs over the AS are smaller in TP100 than in TP00. Whereas the abrupt increase in precipitation occurs in TP00, the large region of precipitation shifts from close to the Equator to the AS more slowly in TP100 during late May to June. Compared to the reduction in geopotential height in the BB, the geopotential height in the AS declines more gradually during April to June. In addition, compared to the reduction in pressure in the AS in TP00, the pressure reduction in the AS in TP100 is more gradual. SSTs above 30°C do not occur during this period in TP100, whereas an SST above 30°C is accompanied by an abrupt depression over the AS in TP00. Thus, the lower SSTs in TP100 are linked to the slow development of low-level pressure fields over the AS. In addition, the precipitable water over the AS in TP100 is less than that in TP00 because the SST is lower under the influence of the TP. The reduced water vapor in TP100 is also associated with the late onset of increased precipitation in the AS under the influence of the TP.

### 4.3. Different SSTs in Adjacent Oceans

[20] The differences in SSTs between TP100 and TP00 likely affect the onset mechanism of the summer monsoon in South Asia. To further demonstrate the relationship between the geographical features and the differences in

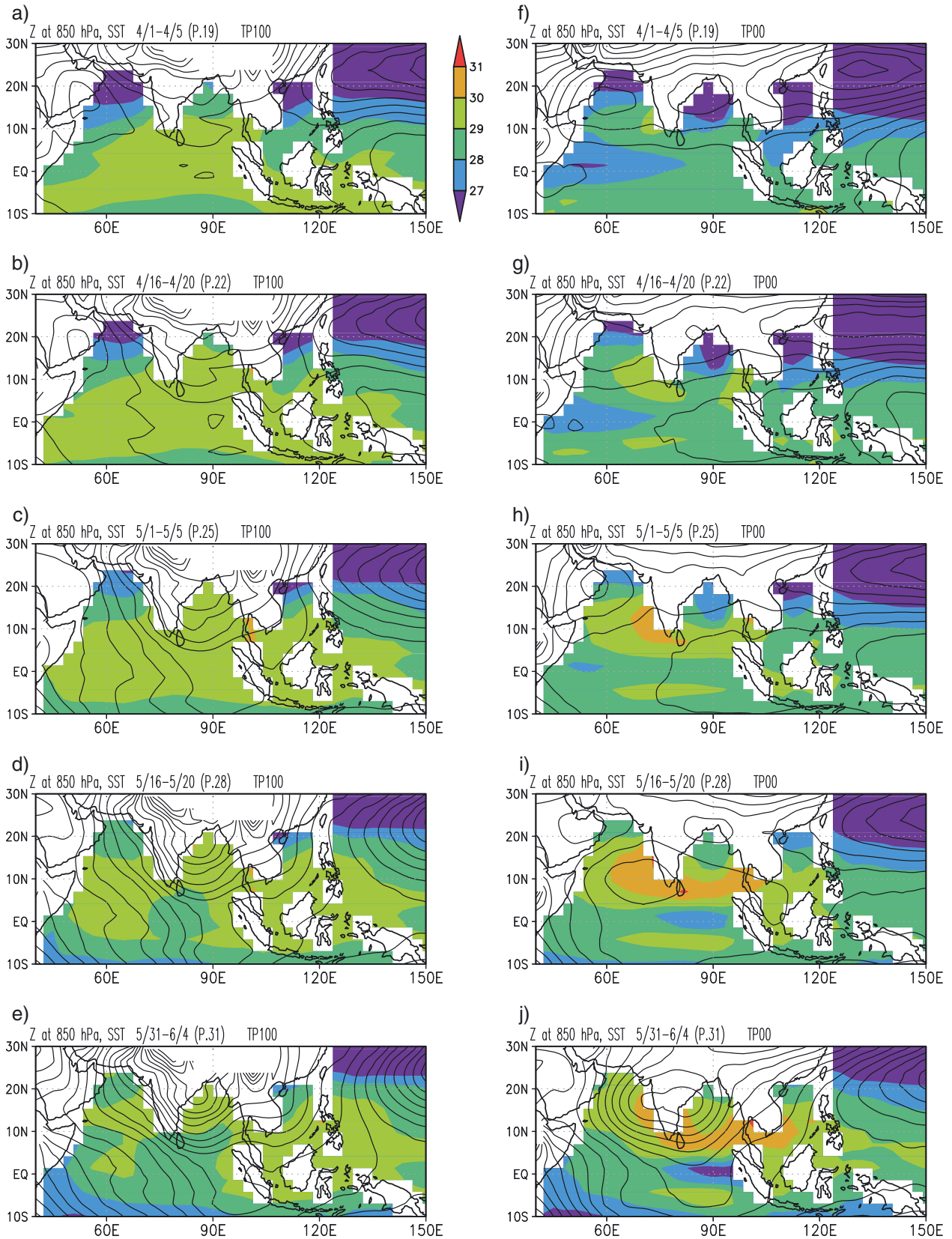


**Figure 10.** Seasonal changes in the spatial distribution of geopotential height (contours) and sea surface temperature (SST) (shade) from TP100 and TP00. The left and right columns are for TP100 and TP00, respectively. Figures from top to bottom in both columns display data for 1–5 April, 16–20 April, 1–5 May, 16–20 May, and 31 May to 4 June. The units of geopotential height and SST are m, kg m/kg s, and °C, respectively. For geopotential height, the data were spatially smoothed to facilitate an understanding of the features of the geopotential heights around the Tibetan Plateau.

SSTs and their seasonal changes, Figure 10 illustrates the seasonal changes in the SST distribution in TP100 and TP00. In the AS during April to June, the SST in TP100 is approximately 1°C lower than that in TP00 (Figures 10i and 10j). The SST difference in the AS between TP100 and TP00 is at its highest in late May. In the BB during April to May, in contrast, the SST in TP100 is approximately 1°C higher than that in TP00, exceeding 29°C in early May.

[21] To illustrate the mechanism that is involved in the differences in SSTs between the two models, Figure 11 illustrates the horizontal and vertical heat transport in the mixed layer between the ocean surface and 30 m depth in TP00 and TP100 in both the first and second halves of May. In the first half of May, in TP100, the southward ocean heat transport from the AS and the BB to the Equator and the upward heat transport in the AS and the BB are induced by a westerly flow caused by the Ekman effect [Webster *et al.*, 1999]. The premonsoon westerly flow is formed as a result of the low-pressure fields south of the TP under the influence of the TP. Thus, colder water from the deeper ocean also contributes lower SSTs in the AS under the influence of the TP. In contrast, in TP00, heat is transported northward from the eastern equatorial Indian Ocean, and there is a weak downward heat transport, which can be attributed to the easterly flow off the Equator that is caused by the subtropical anticyclonic circulation in South Asia during the premonsoon season in the absence of the TP. The northward transport brings warmer water from the Equator to the AS. Therefore, there are remarkable differences in ocean heat transport between TP100 and TP00, as depicted in Figure 10c.

[22] In the second half of May, the distribution of the ocean heat transport in TP100 is quite similar to that in the first half of May. However, in TP00, the ocean heat transport over the western region of the northern Indian Ocean in the second half of May changes in response to the initiation of the monsoon westerly flow in the absence of the TP. The ocean heat transport over the western region of the northern Indian Ocean in TP00 is similar to that in TP100. In addition, upwelling in the AS appears in TP00. Thus, the SST in the AS decreases during the second half of May. In the eastern regions, however, the differences in the heat transport between TP100 and TP00 continue through the second half of May because the westerly flow over the BB and the eastern part of the northern Indian Ocean does not occur in TP00.

[23] In addition, in the BB, the SST during April in TP100 is approximately 2°C higher than in TP00. Figures 10a and 10f show that the difference in SSTs between TP100 and TP00 are distinct. Thus, the higher SST is attributable to the effect of the differences in the air-sea interaction during March and the winter season. During winter, evaporation in the BB in TP100 is lower than that in TP00 due to the weaker easterly under the influence of the TP. Furthermore, because upwelling in the BB is weaker in TP100 during spring and winter, the decrease in the SST is not very great in the BB (data not shown). The increase in SSTs in the eastern part of the BB, which is related to local oceanic circulation within the BB, appears during the premonsoon season. After the onset over the AS, in TP00, a southwesterly appears in the BB and forces the subsurface oceanic water

eastward. This effect results in larger increase in SSTs in the eastern part of the BB.

#### 4.4. Validation of the Effect of the Air-Sea Interaction

[24] To clearly identify the effects of the air-sea interaction on the differences in the timing of the onset of the monsoon season, we conducted AGCM experiments, making two comparisons: AT100 to AT100+O00 and TP00 to AT00. In AT100+O00, the climatological SSTs simulated in TP00 were prescribed. Therefore, the comparison between AT100 and AT100+O00 enabled us to understand the effects of the air-sea interaction that were caused by the presence of the TP. The SSTs prescribed in AT00 are the same climatological SSTs as those simulated in TP100. Thus, a comparison between the results of TP00 and AT00 enabled us to understand effect of the ocean climate under the influence of the TP on the atmosphere with and without the TP.

[25] Figure 12 displays the spatial distribution of the onset date of the South Asian summer monsoon precipitation for AT100, AT00, and AT100+O00. The definition of the onset in the AGCM runs is the same as that in CGCM runs; however, the January mean precipitation in TP100 was substituted for the January mean precipitation of each run to avoid the dependence on different measures of the January mean precipitation. In AT100, the onset date of precipitation for the South Asian summer monsoon is quite similar to that in TP100. In AT100+O00, the onset of precipitation over the AS occurs approximately 15–20 days earlier, because of the higher SST in the AS than in AT100 (TP100). However, remarkable differences in the onset date do not occur in the northern region of the AS and ID because the dry northwesterly flow from west of the TP during the premonsoon seasons suppresses convective activity over the northern region of the AS and ID. In contrast, the onset of the summer monsoon over the BB occurs approximately 15–20 days later because of the lower SST in the BB. The difference in the onset date clearly illustrates that different air-sea interactions strongly affect the onset date of the South Asian summer monsoon.

[26] In AT00, the onset of the monsoon in the AS and the ID, except for the eastern AS, near the southern tip of the Indian Peninsula, differs little from that in AT100, with monsoon precipitation in the AS and the ID beginning in early June. In contrast, the onset in the BB and the Indochina Peninsula in AT00 occur 10 days earlier than in TP00. The earlier onset in the eastern AS, near the southern tip of the Indian Peninsula, in AT00 is also related to the local disturbance that results from spatially higher SSTs that appeared during April. However, this earlier onset of precipitation does not induce the abrupt increase in precipitation over the AS due to the lower SSTs over most regions of the AS and reduced water vapor transport than those in TP00. Figure 6 indicates that the effect of the TP plays a major role in the monsoon onset timing over Southeast and East Asia by forming anticyclonic circulation over the western North Pacific and then enhancing a low-level southwesterly. Therefore, the atmospheric circulation in the presence of the TP has a greater effect on the early onset of the summer monsoon precipitation over the BB and the Indochina Peninsula than on the onset date over the AS and ID. The warming of the adjacent ocean

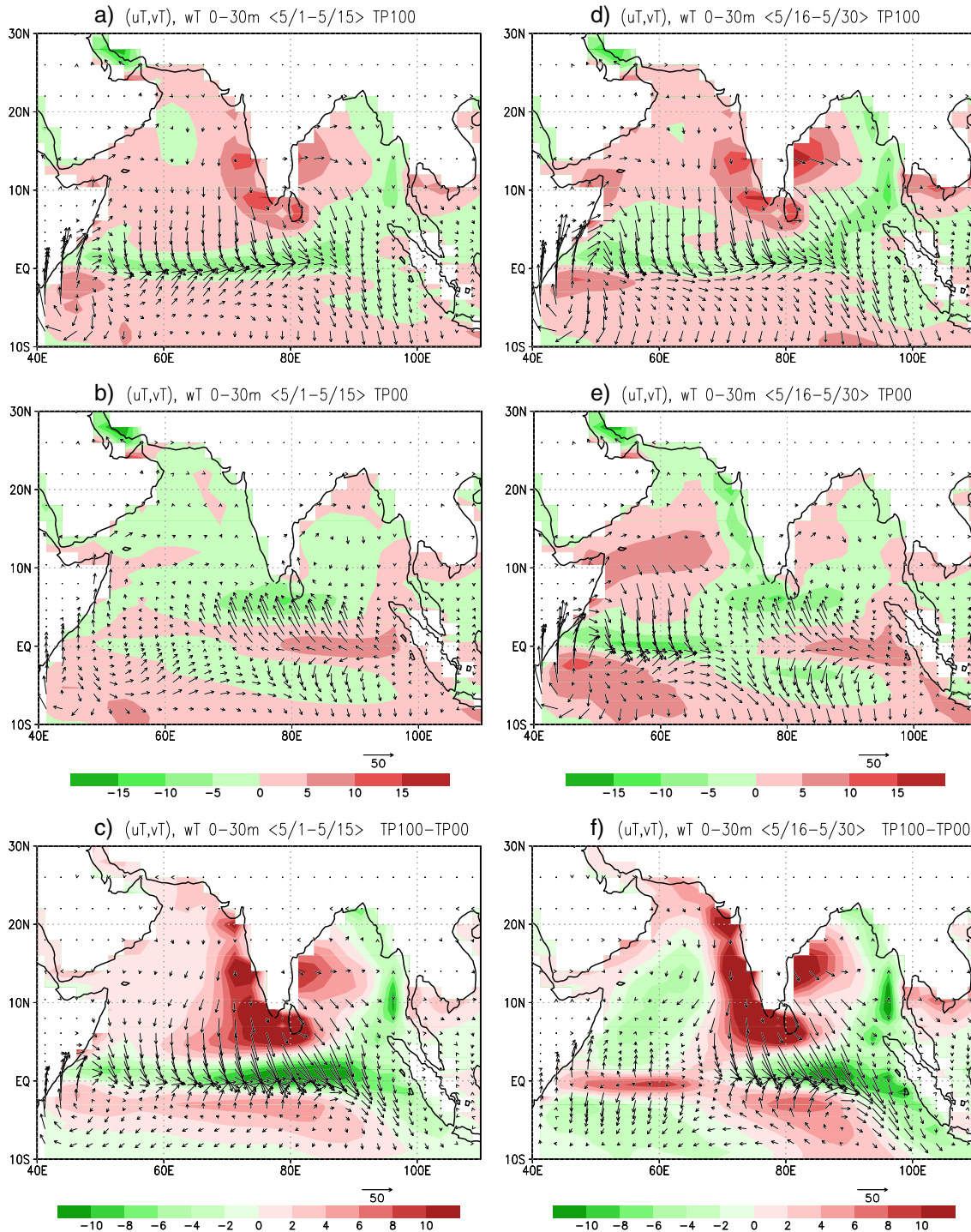


**Figure 11.** Heat transport in the mixed ocean layer between the surface and a depth of 30 m for TP100 and TP00 and the difference between the first and second halves of May. The vector shows the direction of horizontal transport, and the shaded color indicates the vertical transport. The unit is  $\text{K m s}^{-1}$ .

may be a secondary factor for the earlier monsoon onset over the Southeast and East Asia.

[27] Figure 13 illustrates the seasonal changes in the climatological geopotential height and moisture transportation at 850 hPa as well as evaporation minus precipitation ( $E - P$ ) in AT00 and AT100 + O00. During the premonsoon season, low-pressure fields in the south of the TP are found in AT100 + O00, quite similar to those found in the premonsoon

season in AT100 (TP100). However, precipitation in the BB and Indochina Peninsula begins later than that in the AT100. This result can be attributed to the increased stability of the low troposphere and less incoming water vapor due to the lower SST. In the AS, particularly in the southern part, precipitation above  $4 \text{ mm d}^{-1}$  begins earlier than in AT100, concurrently with that in the BB. In the northern region of the AS and the ID, however, a northwesterly flow is formed

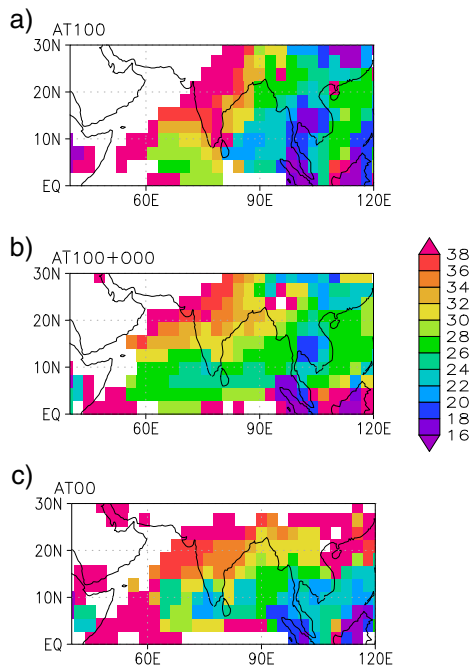


**Figure 12.** A geographical map of the onset date for summer precipitation in AT100 (a), AT100+O00 (b), and AT00 (c). The values represent the pentads numbers for the onset dates.

under the influence of the TP, suppressing the convection. In addition, the surface pressure over the AS decreases more rapidly in AT100+O00 than in AT100 during April to May because the SSTs are higher.

[28] In AT00, before the onset of the monsoon season, the subtropical anticyclonic circulation is found over South Asia, similar to that found in TP00. Therefore, the convective activity in South Asia is also suppressed. However, the abrupt depression over the AS beginning in late April does not occur in AT00 as it does in TP00 because of the lower SSTs in the AS. Thus, the monsoon precipitation in the AS and ID does not begin in AT00 in mid-May. This result clearly indicates that the early onset of the summer monsoon precipitation in the AS and ID in the absence of the TP is attributable to a high SST in the AS and increasing summer precipitation in the ID due to the increased air-sea interaction in the absence of the TP. Over the BB, however, the abrupt depression in AT00 occurs in late May because of the higher SST, and precipitation also increases to initiate monsoon precipitation.

[29] These results from AGCM experiments clearly suggest that the ocean climate, in conjunction with the effect of the TP, causes the early onset of summer monsoon precipitation in the BB and Southeast Asia and the late onset in the AS and ID, both of which are essential features of the current Asian summer monsoon system. Therefore, these results lead to the conclusion that the essential features are modulated by climatological seasonal changes in the ocean, which are significantly altered by the presence of the TP.

## 5. Discussion

[30] *Kanae et al.* [2002] clearly demonstrated that the adjacent warm SST has a more crucial role in the onset of

the summer monsoon on the Indochina Peninsula than the role of the TP. Our results partially support this conclusion; the later onset of the summer monsoon precipitation on the Indochina Peninsula occurs in AT100+O00, with lower SST during April to mid-May than that in AT100 (TP100). However, the warm SST around the Indochina Peninsula during the premonsoon period results from the air-sea interaction in the presence of the TP.

[31] Our results support a low-level instability mechanism for the South Asian monsoon, as proposed by *Minoura et al.* [2003]. Their study revealed a positive, asymmetric SST perturbation before the summer monsoon in the AS and the BB, contributing to both the gradual and earlier onset of the monsoon in the BB and Southeast Asia and the abrupt and later onset in the AS and ID. Our results also suggest that the climatological spatial features that contribute to the contrast between the earlier onset of the monsoon in southeastern Asia and its later onset in southwestern Asia are dominated by the air-sea interaction that is associated with the presence of the TP. Therefore, the low-level instability mechanism may be a more important geographical influence on the onset date than the heating effect of the TP in the middle-upper troposphere.

[32] In several previous studies, global orography was removed [e.g., *Kitoh, 2007; Abe et al., 2003, 2004*]. These studies could not strictly demonstrate the sole effect of the TP on climate because orography other than the TP was considered. The East African highlands, for example, likely contribute to shape of the Somali Jet, which may be related to the onset of the summer monsoon in South Asia [*Chakravorty et al., 2002*]. Thus, the effects of orographic features other than the TP may lead to a difference in results between the present study and previous studies.

[33] The present study clearly reveals that the paleo-ocean change in the AS, which is recorded as sediments of fossil foraminifera, may be strongly associated with a change in the paleo-monsoon circulation pattern due to a change in the air-sea interaction caused by the uplift of the TP. Thus, the AS has experienced several paleo-monsoon changes associated with the uplift of the TP more clearly than other oceans. Using the AGCM, *Boos and Kuang* [2010] suggested that the heating of the TP is less important to intensifying the Asian summer monsoon circulation than the insulating effect of the steep mountain ranges. We could not investigate the effect of narrow orography because of the low resolution of our GCM. However, our study also reveals that the role of convective heating during the evolution of monsoon circulation is important because certain aspects of the monsoon circulation, such as the low-level southwesterly flow, become stronger in conjunction with a greater release of latent heat from the monsoon precipitation in the AS, even in simulations in which the TP is removed. In addition, our results raise the possibility that the Asian summer monsoon circulation would still occur if the TP was not present and that the summer precipitation on the ID without the TP would be greater than that with the TP. This finding adds substantial complexity to an understanding of the variations in the paleo-monsoon circulation that have resulted from the uplift of the TP.

[34] Unfortunately, the coupled GCM has cold biases in SSTs over South Asia, as displayed in Figures 2 and 3. These biases may delay the onset of monsoon precipitation

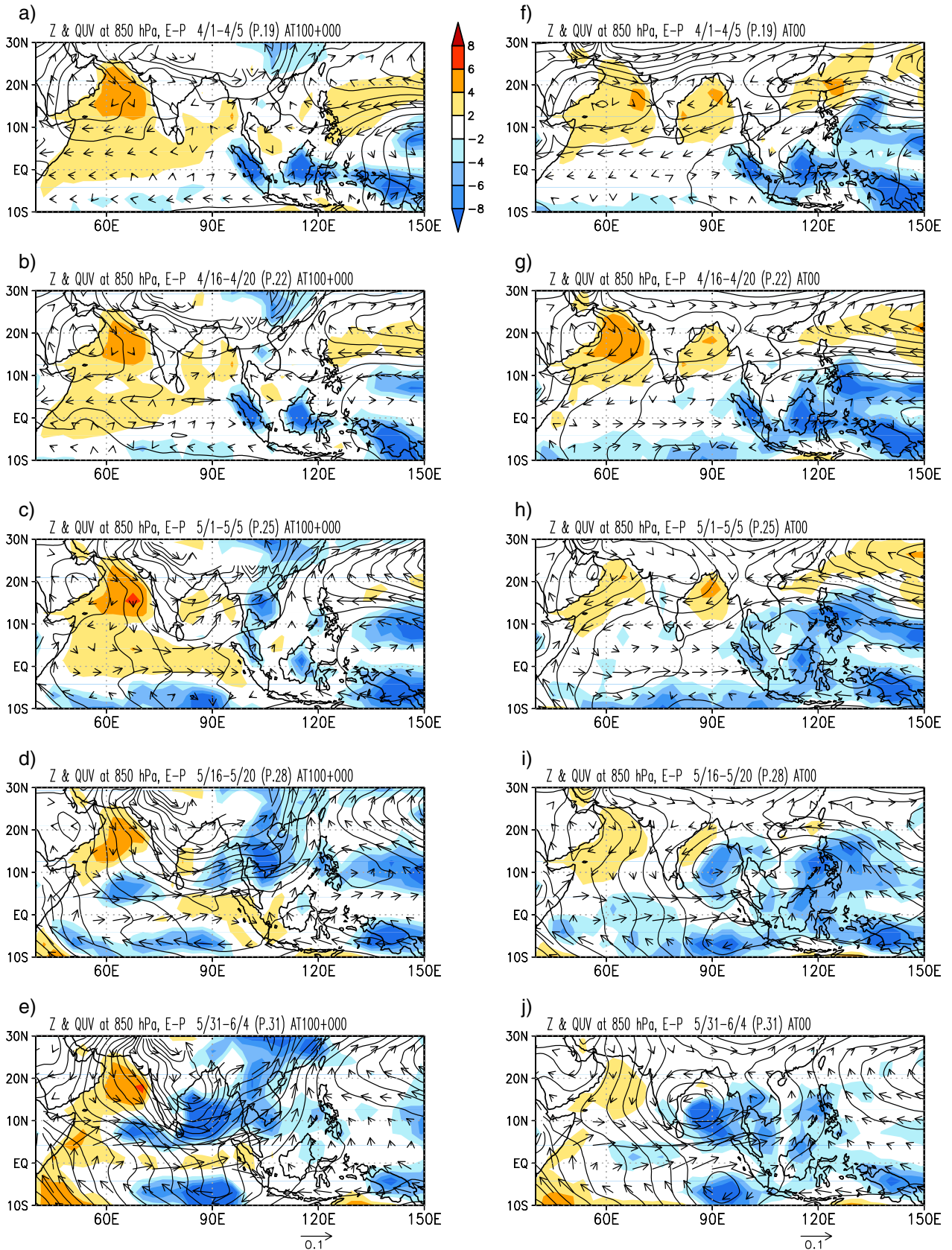


**Figure 13.** Seasonal changes in the spatial distribution of geopotential height (contours), moisture transportation at 850 hPa (vectors), and evaporation minus precipitation ( $E - P$ ) (shading) of AT100+O00 and AT00. Top to bottom in both columns display data for 1–5 April, 16–20 April, 1–5 May, 16–20 May, and 31 May to 4 June. The units of geopotential height, wind, and  $E - P$  are m, kg/m/kg s, and  $\text{mm d}^{-1}$ , respectively.

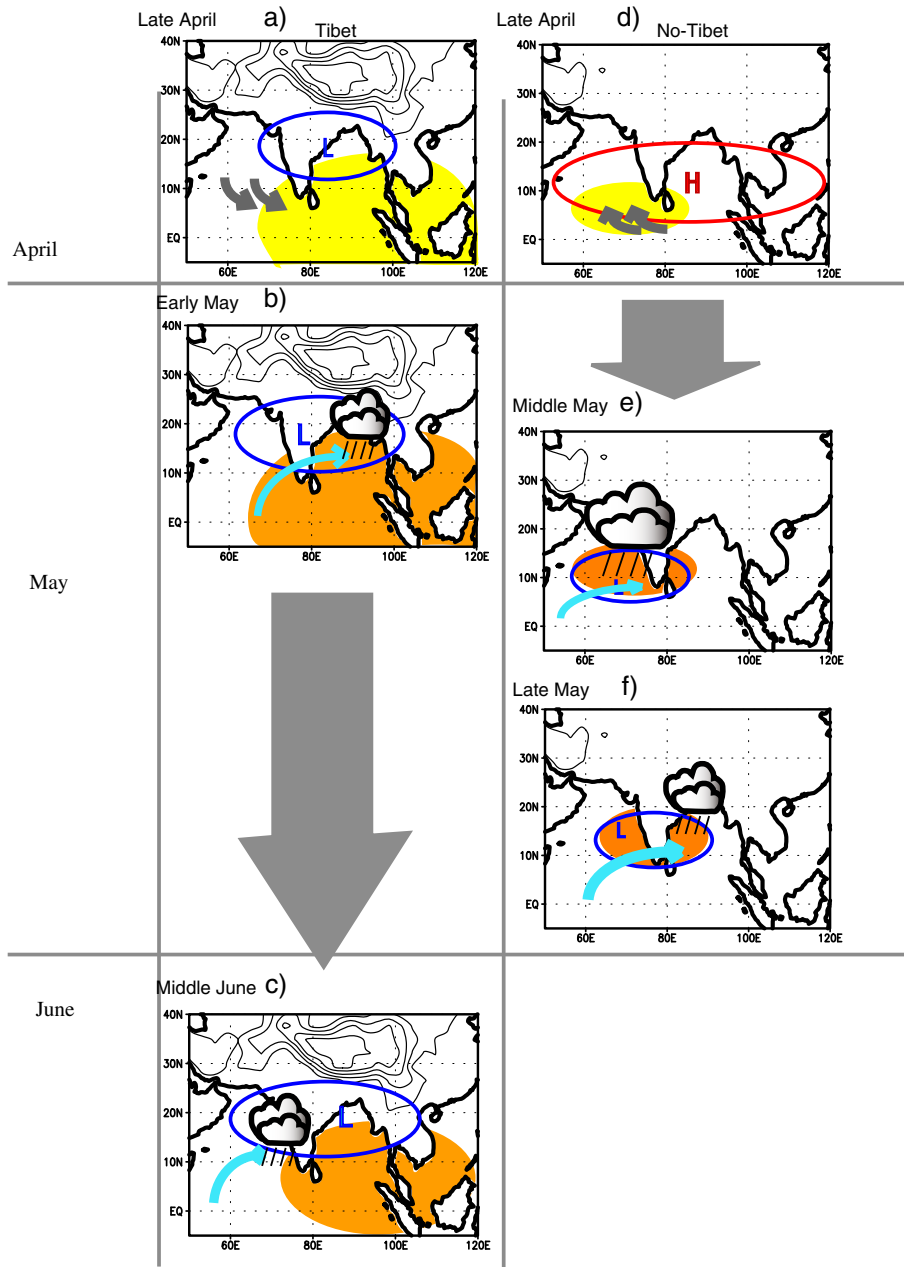


**Figure 14.** A schematic diagram of the onset processes related to the air-sea interactions in TP100 (a, b, c) and TP00 (d, e, f). Red and blue lines indicate atmospheric pressures in the lower troposphere. Yellow and orange colors indicate warmer ocean surface temperatures, with orange indicating a higher temperature than yellow. Light blue arrows indicate the change in the water vapor flow related to the onset. Gray arrows indicate the typical orientation of the subsurface ocean currents. The cloud picture indicates where the summer monsoon precipitation begins.

over the AS and ID. This delayed onset over the AS and ID in TP100 may exaggerate the earlier onset over the AS and ID in TP00. However, as described above, significant differences in the ocean climate between TP100 and TP00 can modulate the onset timing of the summer monsoon over South Asia.

[35] Figure 5 illustrates the delayed onset over South and Southeast Asia, except for the AS, due to the removal of the TP. However, the presence of the TP does not significantly affect the subsequent summer precipitation or the retreat of summer monsoon precipitation in either region.

Thus, due to the TP, the length of the rainy season increases in Southeast Asia and the BB but decreases in the AS and ID in the models used in this study. Understanding why the presence of the TP does not significantly affect the retreat of the summer monsoon would be valuable for future research.

## 6. Summary

[36] Using the GCM, we investigated the effect of the Tibetan Plateau on the onset of South Asian monsoon

precipitation. The coupled atmosphere-ocean GCM experiments indicate that the presence of the TP delays the onset of summer monsoon precipitation in the AS and ID and leads to an earlier onset in the BB. The onset of the South Asian summer monsoon in the presence of the TP is strongly related to the air-sea interaction during the premonsoon season. The lower SSTs in the AS in the presence of the TP are related to the later onset of summer monsoon precipitation in South Asia. In contrast, the simulated SSTs in the BB in the presence of the TP are higher than those in the absence of the TP. Although a significant amount of water vapor is transported to the BB by the southwesterly flow, the higher SSTs contribute to an earlier onset of precipitation in the BB. Therefore, the model experiments demonstrate that the current state of the northern Indian Ocean, including the AS and the BB, modulates the onset mechanism of the South Asian summer monsoon. Figure 14 presents a schematic diagram of the onset processes that are related to the air-sea interactions in both cases. The current SST distribution, such as spatially lower SST in the AS and higher SST in the BB in the premonsoon season, depends on the southward subsurface ocean currents in the southern AS (gray arrows in Figure 14a) and the enhanced upwelling that is created by westerly flows, which are caused by the cyclonic circulation in the presence of the TP during the premonsoon season via the Ekman effect [Webster *et al.*, 1999] (Figure 14a). According to the seasonal progression, SSTs over the northern Indian Ocean increase to contribute actively to the earlier onset of the summer monsoon in the BB (Figure 14b). In contrast, in a scenario without the TP, the anticyclonic circulation in the lower troposphere develops over South Asia during the premonsoon season in late April, inducing the northward subsurface ocean currents north of the Equator (Figure 14d). These currents result in a spatially warmer ocean surface in the AS, which triggers a large depression that initiates summer monsoon precipitation earlier over the AS and the ID (Figure 14e). Finally, the depression develops and initiates the summer monsoon precipitation over the BB (Figure 14f).

[37] With the AGCM runs, we further verified the effect of the air-sea interaction on the difference in the onset times of the monsoon using SSTs in the presence or absence of the TP. The AGCM runs with SSTs in the presence of the TP do not indicate that either the presence or absence of the TP strongly influences the delayed onset of precipitation in the AS or ID, but the absence of the TP causes an earlier onset of precipitation in the BB and Southeast Asia. Furthermore, the AGCM run with SSTs in the absence of the TP demonstrates that the SSTs can change the onset date of the current summer monsoon in Southern Asia; the onset in the AS and ID occur earlier, and that in the BB and Southeast Asia occur later. These results clearly indicate that the geographical features of the onset date of the South Asian summer monsoon are strongly modulated by the climatic conditions in the northern Indian Ocean, including the AS and the BB, resulting from the air-sea interaction in the presence of the TP.

[38] **Acknowledgments.** The authors are grateful to the editor of the *Journal of Geophysical Research-Atmosphere* and two anonymous reviewers for their useful comments. This work was conducted as a

cooperative study between the Hydrospheric Atmospheric Research Center, Nagoya University, and the Meteorological Research Institute and was supported by a grant from the Ministry of Education, Culture, Sports, Science and Technology, Japan (Dynamics of the Sun-Earth-Life Interactive System, No. G-4, the 21st Century COE Program).

## References

- Abe, M., A. Kitoh, and T. Yasunari (2003), An evolution of the Asian summer monsoon associated with mountain uplift—Simulation with the MRI atmosphere-ocean coupled GCM, *J. Meteorol. Soc. Jpn.*, *81*(5), 909–933.
- Abe, M., T. Yasunari, and A. Kitoh (2004), Effects of large-scale orography on the coupled atmosphere-ocean system in the tropical Indian and Pacific Oceans in boreal summer, *J. Meteorol. Soc. Jpn.*, *82*(2), 745–759.
- Bonjean F., and G. S. E. Lagerloef (2002), Diagnostic model and analysis of the surface currents in the tropical Pacific Ocean, *J. Phys. Ocean.*, *32*(10), 2938–2954.
- Boos, W. R., and Z. Kuang (2010), Dominant control of the South Asian monsoon by orographic insulation versus plateau heating, *Nature*, *463*, 14, doi:10.1038/nature08707.
- Chakravorty, A., R. S. Nanjundiah, and J. Srinivasan (2002), Role of Asian and African orography in Indian summer monsoon, *Geophys. Res. Lett.*, *29*, doi:10.1029/2002GL015522.
- Chakravorty, A., R. S. Nanjundiah, and J. Srinivasan (2006), Theoretical aspects of the onset of Indian summer monsoon from perturbed orography simulations in a GCM, *Ann. Geophys.*, *24*, 2075–2089.
- Hahn, D. G., and S. Manabe (1975), The role of mountains in the south Asian monsoon circulation, *J. Atmos. Sci.*, *32*, 1515–1541.
- Inoue and Ueda (2011), Delay of the first transition of Asian summer monsoon under global warming condition, *SOLA*, *7*, 081–084, doi:10.2151/sola.2011-021.
- Kanae, S., T. Oki, and K. Musiaki (2002), Principal condition for the earliest Asian summer monsoon onset, *Geophys. Res. Lett.*, *29*(15), 1764, doi:10.1029/2002GL015346.
- Kutzbach, J. E., P. J. Guetter, W. F. Ruddiman, and W. L. Prell (1989), Sensitivity of climate to late Cenozoic uplift in southern Asia and the American West: Numerical experiment, *J. Geophys. Res.*, *94*, 18,393–18,407.
- Kutzbach, J. E., W. L. Prell, and W. F. Ruddiman, (1993), Sensitivity of Eurasian climate to surface uplift of the Tibetan Plateau, *J. Geol.*, *101*, 177–190.
- Kitoh, A. (1997), Mountain uplift and surface temperature changes, *Geophys. Res. Lett.*, *24*(2), 185–188.
- Kitoh, A. (2004), Effects of mountain uplift on East Asian summer climate investigated by a coupled atmosphere-ocean GCM, *J. Clim.*, *17*(4), 783–802.
- Kitoh, A. (2007), ENSO modulation by mountain uplift, *Climate Dynamics*, *28*, 781–796, doi:10.1007/s00382-006-209-6.
- Li, C. F., and M. Yanai (1996), The onset and interannual variability of the Asian summer monsoon in relation to land sea thermal contrast, *J. Clim.*, *9*(2), 358–375.
- Minoura, D., R. Kawamura, and T. Matsuura (2003), A mechanism of the onset of the South Asian summer monsoon, *J. Meteorol. Soc. Jpn.*, *81*(3), 563–580.
- Okajima, H. and S.-P. Xie (2007), Orographic effects on the northwestern Pacific monsoon: Role of air-sea interaction, *Geophys. Res. Lett.*, *34*, L21708, doi:10.1029/2007GL032206.
- Rajendran, K., A. Kitoh, and S. Yukimoto (2004), South and East Asian summer monsoon climate and variation in MRI coupled model (MRI-CGCM2), *J. Clim.*, *17*, 763–782.
- Reynolds, R. W., N. A. Rayner, T. M. Smith, D. C. Stokes, and W. Wang (2002), An improved in situ and satellite SST analysis for climate, *J. Clim.*, *15*, 1609–1625.
- Shibata, K., H. Yoshimura, M. Ohizumi, M. Hosaka, and M. Sugi (1999), A simulation of troposphere, stratosphere and mesosphere with an MRI/JMA98 GCM, *Pap. Meteorol. Geophys.*, *50*, 15–53.
- Takahashi, H. G., and T. Yasunari (2006), A climatological monsoon break in rainfall over Indochina—A singularity in the seasonal march of the Asian summer monsoon, *J. Clim.*, *19*, 1545–1556.
- Ueda, H., and T. Yasunari (1998), Role of warming over the Tibetan Plateau in early onset of the summer monsoon over the Bay of Bengal and the South China Sea, *J. Meteorol. Soc. Jpn.*, *76*(1), 1–12.
- Uppala, S. M., et al. (2005), The ERA-40 re-analysis, *Q. J. R. Meteorol. Soc.*, *131*(612), 2961–3012, doi:10.1256/qj.04.176.
- Yukimoto, S., A. Noda, A. Kitoh, M. Sugi, Y. Kitamura, M. Hosaka, K. Shibata, S. Maeda, and T. Uchiyama (2001), The New

- Meteorological Research Institute Coupled GCM (MRCGCM2)—model climate and variability, *Pap. Meteorol. Geophys.*, 51(2), 47–88.
- Wang, B., and LinHo (2002), Rainy season of the Asian-Pacific summer monsoon, *J. Clim.*, 15, 386–398.
- Webster, P. J., A. Moore, J. P. Loschnigg, and R. R. Leben (1999), Coupled ocean-atmosphere dynamics in the Indian Ocean during 1997–98, *Nature*, 401, 356–360, doi:10.1038/43848.
- Wu, G. X., and Y. S. Zhang (1998), Tibetan Plateau forcing and the timing of the monsoon onset over South Asia and the South China Sea, *Mon. Wea. Rev.*, 126(4), 913–927.
- Xie, P. P., and P. A. Arkin (1997), Global precipitation: A 17-year monthly analysis based on gauge observations, satellite estimates, and numerical model outputs, *Bull. Amer. Meteorol. Soc.*, 78(11), 2539–2558.